Journal of Pharmaceutical and Biomedical Analysis 51 (2010) 979–984

Contents lists available at ScienceDirect

Journal of Pharmaceutical and Biomedical Analysis

journal homepage: www.elsevier.com/locate/jpba

Short communication

Thermal conductivity measurements for small molecule organic solid materials using modulated differential scanning calorimetry (MDSC) and data corrections for sample porosity

Yannan Lin [a], Zhenqi Shi [b], Peter L.D. Wildfong [b,*]

[a] Fujian Health College, 366 Jinxi, Minhou County, Fuzhou, Fujian Province, 350101, China
[b] Duquesne University Graduate School of Pharmaceutical Sciences, 600 Forbes Ave., Pittsburgh, PA 15282, United States

ARTICLE INFO

Article history:
Received 23 July 2009
Received in revised form 22 October 2009
Accepted 23 October 2009
Available online 5 November 2009

Keywords:
Thermal conductivity
Pharmaceutical small molecule organic materials
Porosity
Zero-porosity extrapolation
Modulated differential scanning calorimetry

ABSTRACT

A method for measuring the thermal conductivity (k) of small molecule organic solid materials using modulated differential scanning calorimetry (MDSC) is demonstrated. Sample preparation required powder consolidation, unavoidably introducing air voids into compacts. Supporting equations for the technique were modified to include a porosity term (ε), and the theoretical quadratic relationship between k and ε was confirmed by experimental measurements for 18 representative materials. Zero-porosity extrapolation was used to approximate values of "true" thermal conductivity for non-porous solids ($k_{\varepsilon=0}$). Zero-porosity-extrapolated values ranged from 0.1273 W/(K m) to 0.3472 W/(K m) for all materials, consistent with expected values of k for non-porous organic polymers.

1. Introduction

Thermal conductivity (k) is a fundamental property that represents the ability of a material to transfer heat across a temperature gradient. Metals, whose internal structures consist of numerous free electrons, tend to be extremely good thermal conductors, having k values that typically range from 20 to 400 W/(K m) [1]. In contrast, nonmetallic materials, which rely on phonon propagation for less efficient heat transfer, have k values that range from 2 to 50 W/(K m) for ceramic materials [1], and fall on the order of 0.3 W/(K m) for organic polymers [1,2]. Small molecule organic solids, typical of active pharmaceutical ingredients (API) and excipients, are expected to have k values similar in magnitude to organic polymers.

Models that demonstrate material responses to processing environments, as well as those that facilitate prediction and minimization of potential thermal effects during storage, handling and shipping, are important in keeping with 21st century development of pharmaceutical drug products. Thermal conductivity was identified as an essential parameter in investigations of temperature effects involved in solid phase transformations during high shear impact milling [3,4], as well as important to modeling temperature evolution during compaction of pharmaceutical powders [5,6]. In either case, establishing whether or not heat transfer results in a temperature excursion capable of causing a deleterious phase change, or chemical degradation is an important aspect of helping to ensure product quality. In the milling work, k had to be approximated based on measurements in organic polymers, owing to the rarity of reported values for pharmaceutically relevant materials. This paucity of thermal conductivity data for pharmaceutical materials makes accurate measurement of this property important.

Diverse experimental techniques have been used to measure k [2,7–17], employing methodologies, equipment, sample sizes, and experimental time scales that lend themselves differently to measurement capability, particularly for pharmaceutically relevant materials. Methods that utilize differential scanning calorimetry (DSC) instrumentation provide rapid measurement of k in the context of a common, commercially available instrument, ubiquitously present in pharmaceutical characterization laboratories. Adaptations of different DSC instruments for measurements of k have been carried out by various groups [2,10–13,16,17]; some methods hold the disadvantage of specially designed accessories or modifications to the DSC cell [2,11,17], while others are inappropriate owing to

* Corresponding author at: Duquesne University Graduate School of Pharmaceutical Sciences, Mellon Hall 422C, 600 Forbes Ave., Pittsburgh, PA 15282, United States. Tel.: +1 412 396 1543; fax: +1 412 396 4660.
E-mail address: wildfongp@duq.edu (P.L.D. Wildfong).

0731-7085/$ – see front matter © 2009 Elsevier B.V. All rights reserved.
doi:10.1016/j.jpba.2009.10.022

the low melting points of small molecule solids relative to available metallic standards [12,16].

MDSC extends conventional DSC, and can be used to measure k for small molecule organic materials without the experimental limitations described above. MDSC employs a sinusoidal temperature variation, which is superimposed on a linear temperature ramp. This feature allows separation of the total heat flow signal into its reversing (thermodynamic, heat capacity-related) and non-reversing (kinetic) components [18,19]. Direct measurement of heat capacity is then used to determine k. Although MDSC methods have been used to measure k for inorganic solids and polymer films [20,21], applications of this technique for pharmaceutical solids have not been reported.

Sample preparation involving small molecule organic solid materials requires consolidation as un-sintered powder compacts (as opposed to cast films or ingots). The unavoidable presence of air-filled voids within a sample creates a solid–vapor two-phase composite, whose overall k will be influenced by the low thermal conductivity of air (~0.02 W/(K m)). The inorganic materials literature has demonstrated that the presence of pores in a solid scatters phonons as they move through a material, effectively decreasing their mean free path of transport [22,23]. Equations derived from fundamental equations of phonon transport, however, substantially overestimate experimental measurements of thermal conductivity relative to pore fraction [22].

Given the relationship between void fraction and thermal conductivity, it is noted that pharmaceutically relevant raw materials, process intermediates, and solid drug products will invariably contain some ε, potentially rendering models that use unadjusted values of k less accurate. The objective of this study was, therefore, to demonstrate the need for correcting experimentally determined k measurements based on ε. A theoretical quadratic relationship is derived, and zero-porosity extrapolation is used to approximate "true" values of thermal conductivity for non-porous crystals.

2. Theory

Blain and Marcus derived Eq. (1) to determine the observed thermal conductivity (k_o, W/(K m)) of right cylinder samples using MDSC [18,20]:

$$k_o = \frac{8LC^2}{C_p M d^2 P} \tag{1}$$

Here, L is the sample thickness (mm), C the apparent heat capacity (mJ/K), C_p the specific heat capacity (J/(g K)), M the specimen mass (mg), d the specimen diameter (mm) and P the period of measurement (s). The porosity of a powder column is a fractional quantity defined by Eq. (2):

$$\varepsilon = 1 - \frac{\rho_A}{\rho_{cryst}} \tag{2}$$

where ρ_{cryst} is the density of the solid material based on its crystallographic structure (true density), calculated using Eq. (3):

$$\rho_{cryst} = \frac{m_w Z}{0.60221 V} \tag{3}$$

where m_w is the molecular weight of the molecule, Z is the number of crystallographically unique molecules in the unit cell of the crystal structure, and V is the unit cell volume (Å^3) [24]. Although not presented in the current work, in the absence of crystallographic data for a given material, or in the case of non-crystalline solids, ρ_{cryst} could be experimentally determined using helium pycnometry.

The apparent density, ρ_A, used in Eq. (2) is easily calculated assuming a right cylinder solid specimen:

$$\rho_A = \frac{4M}{\pi d^2 L} \tag{4}$$

Variables in Eq. (4) are the same as those for Eq. (1).

While L, C_p, d, ρ_{cryst}, and P are constants for any experiment, C and M will vary with respect to ε. Combination of Eqs. (2) and (4) and substitution into Eq. (1), shows a quadratic relationship between k_o and ε (see Appendix A)[1]:

$$k_o(\varepsilon) = \frac{32}{\pi C_p d^4 P \rho_{cryst}} \cdot \frac{C^2(\varepsilon)}{(1-\varepsilon)} \tag{5}$$

Zero-porosity extrapolation of k data measured over a range of ε allows approximation of a "true" thermal conductivity representative of k for the non-porous crystal ($k_{\varepsilon=0}$). Although the porosity of a powder column can vary with particle size distribution (*i.e.*, pore volume and specific microstructure will be related to surface area), neither particle size nor specific surface area was used as an additional variable in the present work to correct measurements of k. The reasons are considered as follows: first, particle size distribution only helps describe interparticulate pores, while porosity encompasses both inter- and intraparticulate pores. Thus, porosity is expected to better characterize air-filled voids both within and among powder particles than an explicit particle size distribution or specific surface area. Second, since porosity is partially dependent on particle size, adding an aliasing factor into Eq. (4) is expected to induce difficulty when regression is used to explore the quadratic relationship. Ultimately, more specific measurements of pore volume and microstructure represent a logical expansion of the present data and will be pursued in future work.

3. Experimental

3.1. Materials

High-purity samples of 18 separate materials were purchased for use (Table 1); all chemicals were used as received, with exceptions described below. Phase purity of all materials was confirmed using X-ray powder diffraction (XRPD) by comparison of experimental data with known structures obtained from the Cambridge Structural Database (CCDC) [25–27]. For consistency of sample preparation, the median particle size (d_{50}) of each material was measured by sieve analysis, and is reported in Table 2. XRPD and DSC were used to evaluate sized samples; neither the diffraction patterns nor the thermal traces showed any evidence of disordering upon sample preparation of either sample. Theophylline monohydrate was prepared in-house by storing anyhydrous theophylline for 1 week in a desiccator maintained at 75% relative humidity and room temperature. Phase purity was confirmed by comparison of experimental XRPD patterns with the known diffraction pattern (CCDC reference code: *THEOPH*) [25–27]. Confirmation of the monohydrate was also performed using thermogravimetric analysis (TGA); consistent with the theoretical value, the water content of theophylline monohydrate determined by TGA was 9.1% (w/w). Polystyrene (PS) and poly(methyl methacrylate) (PMMA) standards were used as conductivity reference materials (see Section 3.4 for description).

3.2. Thermal instrumentation

A TA Instruments Q100 heat flux DSC, temperature-controlled using a refrigerated cooling accessory (TA Instruments, New Castle,

[1] Eq. (5) is algebraically equivalent to Eq. (3) reported in [3].

Table 1
Linear dependence of $C(\varepsilon)$ (mJ/K) for 18 small molecule organic solids at 25 °C.

Material	Source	$C(\varepsilon)$ (mJ/K)	R^2
Acetaminophen	Sigma–Aldrich	$C(\varepsilon) = -82.508\varepsilon + 57.412$	0.9633
Aspirin	Sigma–Aldrich	$C(\varepsilon) = -93.097\varepsilon + 61.843$	0.9747
Carbamazepine III	Acros	$C(\varepsilon) = -115.950\varepsilon + 70.578$	0.9861
γ-Indomethacin	Sigma–Aldrich	$C(\varepsilon) = -72.925\varepsilon + 53.429$	0.9889
Ketoprofen	MP Biomedicals	$C(\varepsilon) = -62.078\varepsilon + 53.663$	0.9734
β-D-Lactose	Acros	$C(\varepsilon) = -146.140\varepsilon + 79.001$	0.9864
α-D-Lactose·1H_2O	Acros	$C(\varepsilon) = -109.690\varepsilon + 79.810$	0.9754
β-D-Mannitol	Acros	$C(\varepsilon) = -98.801\varepsilon + 76.180$	0.9834
Naproxen	Fluka Chimie	$C(\varepsilon) = -70.239\varepsilon + 50.405$	0.9812
β-Piroxicam	MP Biomedicals	$C(\varepsilon) = -93.333\varepsilon + 57.996$	0.9827
Salicylamide	Sigma–Aldrich	$C(\varepsilon) = -182.200\varepsilon + 75.104$	0.9630
β-Sulfanilamide	Acros	$C(\varepsilon) = -63.875\varepsilon + 69.014$	0.9870
Sulfathiazole III	Alfa Aesar	$C(\varepsilon) = -78.599\varepsilon + 60.067$	0.9783
Sucrose	Sigma–Aldrich	$C(\varepsilon) = -145.220\varepsilon + 77.482$	0.9855
Theophylline	BASF	$C(\varepsilon) = -77.803\varepsilon + 59.260$	0.9616
Theophylline·1H_2O		$C(\varepsilon) = -112.540\varepsilon + 75.813$	0.9809
Trehalose	Acros	$C(\varepsilon) = -130.310\varepsilon + 86.170$	0.9905
Tolbutamide I	MP Biomedicals	$C(\varepsilon) = -59.217\varepsilon + 54.858$	0.9789

DE) was used for all MDSC measurements. The furnace was continuously purged with N_2 gas (50 mL/min), and a three-point temperature and enthalpy calibration was carried out at 10 °C/min using Sn, In, and *o*-terphenyl as standard references. The instrument was calibrated for heat capacity in modulated mode, using a sapphire standard.

3.3. Measurement of specific heat capacity (C_p) and apparent heat capacity (C)

Specific heat capacity was measured for each material using MDSC and "thin" compacts. Powders were consolidated in a 6 mm evacuable pellet die (Reflex Analytical) using a Carver 3887 AutoPellet hydraulic press (Carver, Inc., Wabash, IN) over a 10 s dwell time to a controlled thickness (0.4 ± 0.1 mm) to ensure uniform temperature distribution during modulation. Compacts were encapsulated in standard DSC aluminum sample pans (Fig. 1a), and isothermally equilibrated in the DSC furnace at 25 °C for 20 min, using a temperature modulation with a fixed amplitude and period (±0.5 °C; 80 s). Values for C_p were obtained by normalizing the measured heat capacity of the specimen to its mass, and reported as the mean value of triplicate samples (Table 2).

Apparent heat capacity of porous samples was obtained from measurements on "thick" specimens (3.5 ± 0.5 mm), where L was controlled to ensure a consistent inter-sample temperature gradient during temperature modulation (Table 2). Specimens having different ε were prepared using the 6 mm evacuable pellet die and press indicated above (for forces above 9.0 kN) and a manual Carver 3851 bench top hydraulic press (Carver, Inc., Wabash, IN) for forces below 9.0 kN. Compaction dwell times were 10 s, while forces were varied between 2.2 kN and 15.6 kN. The dimensions of each compact were measured immediately prior to MDSC measurements to avoid errors attributable to compact elastic relaxation. A drop of silicon oil was placed on the DSC sample sensor platform, on top of which a thin aluminum foil disk was added to facilitate effective thermal contact between platform and specimen. To balance thermal effects, an equivalent foil disk and silicon oil droplet was placed on the reference sensor. Test specimens were placed on top of the foil disk (Fig. 1b), and the samples were subjected to the same temperature modulation as the "thin" specimens. It has been suggested that silicon added to both sides of the aluminum foil disks maximizes effective thermal contact between the DSC platform and the materials [21]. This recommendation, however, assumes non-porous specimens, and is, therefore unsuitable for the present work given that porous compacts will absorb the silicon oil. As such, test specimens were placed in the furnace in direct contact with the upper side of the aluminum foil.

Table 2
CCDC reference codes, ρ_{cryst}, d_{50}, C_p and L data for 18 small molecule organic solids.

Material	CCDC *Refcode*[a]	ρ_{cryst} (g/cm^3)[a]	d_{50} (μm)	C_p (J/(g K)) (±sd, n = 3)	L (mm) (±sd, n = 12)
Acetaminophen	*HXACAN01*	1.293	183	1.289 (0.005)	3.542 (0.061)
Aspirin	*ACSALA01*	1.401	188	1.136 (0.006)	3.473 (0.109)
Carbamazepine III	*CBMZPN01*	1.347	360	1.189 (0.030)	3.428 (0.104)
γ-Indomethacin	*INDMET*	1.372	76	1.165 (0.004)	3.518 (0.058)
Ketoprofen	*KEMRUP*	1.284	370	1.197 (0.029)	3.555 (0.051)
β-D-Lactose	*BLCATO*	1.586	105	1.180 (0.005)	3.517 (0.020)
α-D-Lactose·1H_2O	*LACTOS10*	1.530	155	1.167 (0.018)	3.538 (0.038)
β-D-Mannitol	*DMANTL07*	1.484	89	1.288 (0.009)	3.543 (0.035)
Naproxen	*COYRUD*	1.266	239	1.273 (0.009)	3.425 (0.139)
β-Piroxicam	*BIYSEH*	1.475	183	1.203 (0.007)	3.517 (0.047)
Salicylamide	*SALMID*	1.346	94	1.277 (0.002)	3.495 (0.014)
β-Sulfanilamide	*SULAMD03*	1.514	104	1.220 (0.020)	3.459 (0.091)
Sulfathiazole III	*SUTHAZ02*	1.569	97	0.987 (0.027)	3.522 (0.091)
Sucrose	*SUCROS03*	1.590	329	1.243 (0.003)	3.571 (0.072)
Theophylline	*BAPLOT01*	1.493	175	1.064 (0.019)	3.518 (0.109)
Theophylline·1H_2O	*THEOPH*	1.458	81	1.176 (0.005)	3.488 (0.043)
Trehalose	*YOXFUM*	1.636	101	1.171 (0.017)	3.524 (0.049)
Tolbutamide I	*ZZZPUS02*	1.247	174	1.466 (0.020)	3.505 (0.058)

[a] Please see Refs. [25–27] for acknowledgement of access to the CCDC.

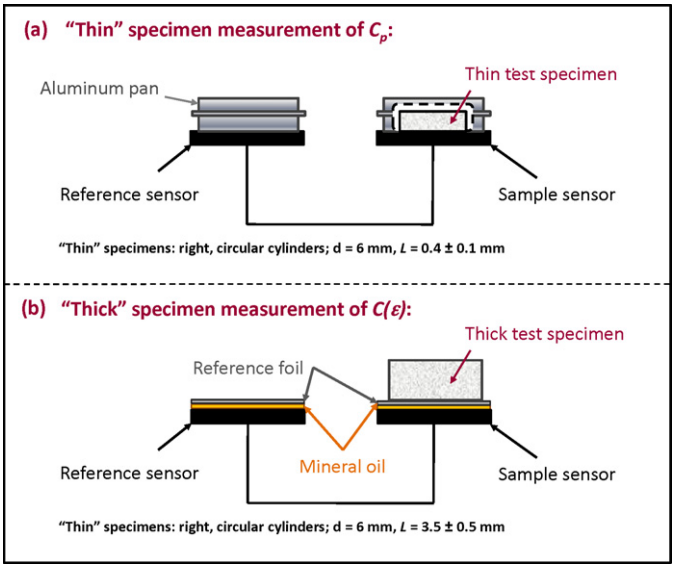

Fig. 1. (a) C_p measurements using MDSC and "thin" specimens and (b) $C(\varepsilon)$ measurement using MDSC and "thick" samples varied over ε.

3.4. Thermal conductivity (k) as a function of sample porosity (ε)

The thermal conductivity constant (D) was calculated to correct heat losses through the surrounding purge gas [18,20] using Eq. (6). Non-porous, cast PS specimen disks, having $d = 6.35$ mm and L of either 0.4 mm (thin standard; C_p) or 3.5 mm (thick standard; C) were used to determine D:

$$D = (k_{o,PS} \cdot k_{r,PS})^{1/2} - k_{r,PS} \quad (6)$$

where $k_{o,PS}$ is determined for non-porous PS using Eq. (1), while $k_{r,PS}$ is the PS reference value at 25 °C (0.1536 W/(K m)). Measured values of D uniformly fell within the range reported to be physically meaningful (0.0100–0.0500 W/(K m)) [21]. For all materials, at each ε, Eq. (5) was used to determine k_o, and corrected using D to obtain the thermal conductivity (k) of any sample (Eq. (7)) [18,20,21]:

$$k = \frac{1}{2} \cdot \left[k_o - 2D + \sqrt{k_o^2 - 4Dk_o} \right] \quad (7)$$

Technique accuracy was determined by repeating MDSC measurements using non-porous, cast PMMA disk specimens as a reference. Like the PS reference specimens, PMMA reference disks had a diameter of 6.35 mm, and a thickness of either 0.4 mm (thin standard; C_p) or 3.5 mm (thick standard; C). The values of k for PMMA using the same procedure were determined to be within 1.1% of the reference value [21].

4. Results and discussion

As shown in Eq. (5), determination of the functionality of $C(\varepsilon)$ was necessary. Linear functions for each material were interpolated from measurements of C *vs.* ε (Table 1). It is noted that the linearity of $C(\varepsilon)$ is better for some materials than for others. This is a reflection of the unavoidable variability inherent to preparation of compacts from pharmaceutical powders, where consolidation is highly dependent on material response to the transfer of a physical load across a powder bed during axial compaction. It is anticipated, therefore, that poorly compactible materials such as acetaminophen may demonstrate greater variability in porosity, density, and interparticulate bond anisotropy relative to easily compacted materials, which contributes to inconsistent heat transfer across the samples. Additionally, variability in particle size and particle size distribution can change the specific microstructure of the compacts; as such sample preparation should utilize consistently sized materials.

Experimental values for k were obtained from measurements on twelve separate samples for each material. The lower ε boundary was determined by the physical limitations of compact preparation (*i.e.*, the lowest ε obtainable by consolidation at maximum compaction force). Likewise, the upper limit for ε was established by application of the minimum compaction force required to produce a physically integral compact. The predicted quadratic relationship between k and ε (see Appendix A), is plotted in Fig. 2 relative to data collected for trehalose. The root mean square error (RMSE) was determined for each dataset relative to the theoretical quadratic model (see Appendix A, Eq. (A.9)), all of which indicate very good agreement between theory and experimentally determined values (Table 3). The thermal conductivities of fully dense samples of each material were imputed by model extrapolation to zero porosity. Values of $k_{\varepsilon=0}$ for all 18 materials were determined to range between 0.1273 and 0.3472 W/(K m), consistent with values observed for non-porous organic polymers.

The method described herein provides a means by which the thermal conductivity of small molecule organic solid materials can be measured using a commonly available technique (MDSC). As accurate determination of k relies upon measurement of C, and C_p, it is recommended that regular calibration for these parameters be

Table 3
Quadratic dependence of $k(\varepsilon)$ (W/(K m)) for 18 small molecule organic solids, and respective values for $k_{\varepsilon=0}$.

Material	$k(\varepsilon)$ (W/(K m))[a]	RMSE (W/(K m))	$k_{\varepsilon=0}$ (W/(K m))
Acetaminophen	$k(\varepsilon) = 0.0482\varepsilon^2 - 0.3567\varepsilon + 0.1659$	0.0036	0.1659
Aspirin	$k(\varepsilon) = 0.0867\varepsilon^2 - 0.4702\varepsilon + 0.2089$	0.0058	0.2089
Carbamazepine III	$k(\varepsilon) = 0.1889\varepsilon^2 - 0.6866\varepsilon + 0.2741$	0.0047	0.2741
γ-Indomethacin	$k(\varepsilon) = 0.0272\varepsilon^2 - 0.2969\varepsilon + 0.1474$	0.0020	0.1474
Ketoprofen	$k(\varepsilon) = 0.0032\varepsilon^2 - 0.2359\varepsilon + 0.1558$	0.0045	0.1558
β-D-Lactose	$k(\varepsilon) = 0.3599\varepsilon^2 - 0.8831\varepsilon + 0.2988$	0.0060	0.2988
α-D-Lactose·1H_2O	$k(\varepsilon) = 0.0746\varepsilon^2 - 0.6045\varepsilon + 0.3211$	0.0059	0.3211
β-D-Mannitol	$k(\varepsilon) = 0.0386\varepsilon^2 - 0.4686\varepsilon + 0.2700$	0.0031	0.2700
Naproxen	$k(\varepsilon) = 0.0242\varepsilon^2 - 0.2710\varepsilon + 0.1273$	0.0047	0.1273
β-Piroxicam	$k(\varepsilon) = 0.0888\varepsilon^2 - 0.4055\varepsilon + 0.1579$	0.0046	0.1579
Salicylamide	$k(\varepsilon) = 0.8673\varepsilon^2 - 1.2239\varepsilon + 0.2905$	0.0051	0.2905
β-Sulfanilamide	$k(\varepsilon) = 0.0015\varepsilon^2 - 0.2099\varepsilon + 0.2234$	0.0046	0.2234
Sulfathiazole III	$k(\varepsilon) = 0.0293\varepsilon^2 - 0.3615\varepsilon + 0.1996$	0.0049	0.1996
Sucrose	$k(\varepsilon) = 0.3386\varepsilon^2 - 0.8108\varepsilon + 0.2673$	0.0051	0.2673
Theophylline	$k(\varepsilon) = 0.0280\varepsilon^2 - 0.3449\varepsilon + 0.1881$	0.0055	0.1881
Theophylline·1H_2O	$k(\varepsilon) = 0.1162\varepsilon^2 - 0.6353\varepsilon + 0.2974$	0.0099	0.2974
Trehalose	$k(\varepsilon) = 0.2100\varepsilon^2 - 0.7719\varepsilon + 0.3472$	0.0060	0.3472
Tolbutamide I	$k(\varepsilon) = -0.0018\varepsilon^2 - 0.1830\varepsilon + 0.1341$	0.0049	0.1341

[a] *Note*: All predicted quadratic functions $k(\varepsilon)$ had $R^2 = 1.0000$.

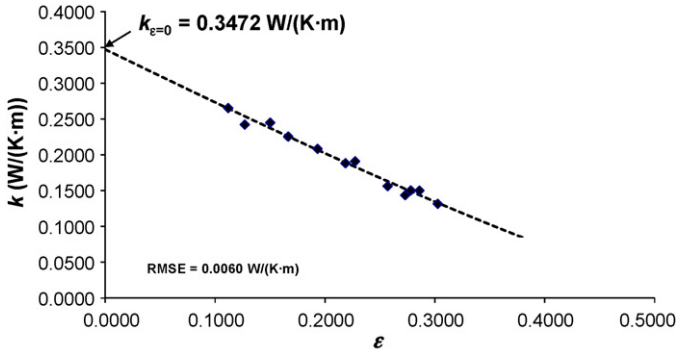

Fig. 2. Thermal conductivities of trehalose (♦) as a function of porosity, plotted relative to theory (- - -). Zero-porosity-extrapolated thermal conductivity ($k_{\varepsilon=0}$) and RMSE of experimental data relative to theory are indicated.

done according to the regularity of instrument use and vendor specifications. This technique is anticipated to be easily implemented with new materials for which limited characterization data are known, as the only input parameter needed (outside of sample dimensions and mass) is the crystallographic density, which is easily obtained given a known crystal structure. Consistent sample preparation is essential to accurate measurement, which may be affected by pore volume and pore surface area as they relate to the particle size and particle size distribution of materials. These elements of specific microstructure require further consideration, and represent a future extension of this work.

5. Conclusions

A method for the measurement of the thermal conductivity of pharmaceutical small molecule organic solids was developed using MDSC. The thermal conductivities of 18 pharmaceutical solid materials were measured at room temperature and the theoretical quadratic dependence of k on ε was confirmed. Zero-porosity extrapolation was used to estimate $k_{\varepsilon=0}$ values for non-porous crystals; all values were determined to fall within an acceptable range consistent with the type of materials under consideration. The present data are believed to represent the most comprehensive list of k values reported for pharmaceutically relevant materials as determined by a single technique, in addition to the first report to specifically address variations in this measurement as a function of sample microstructure.

Acknowledgements

The authors wish to acknowledge the use of the Chemical Database Service at Daresbury and the Cambridge Center for Crystallographic Data. Additionally, the authors wish to acknowledge Colleen Hair and Satya Avula for their assistance with data collection.

Appendix A. Quadratic dependence of $k(\varepsilon)$

Manuscript Eq. (1) relates k_o to MDSC sample physical constants L, C, C_p, M, d, and P:

$$k_o = \frac{8LC^2}{C_p M d^2 P} \tag{A.1}$$

Manuscript Eqs. (2) and (3) (respectively for ε and ρ_A) are combined and rearranged to relate $M(\varepsilon)$:

$$M(\varepsilon) = \frac{(1-\varepsilon)\pi d^2 L \rho_{cryst}}{4} \tag{A.2}$$

As both M and C vary with ε, substitution of Eqs. (A.1) and (A.2) relates k_o to ε:

$$k_o(\varepsilon) = \frac{32}{C_p P \pi \rho_{cryst} d^4} \cdot \frac{C^2(\varepsilon)}{(1-\varepsilon)} = \varphi \cdot \frac{C^2(\varepsilon)}{(1-\varepsilon)} \tag{A.3}$$

$C(\varepsilon)$ is experimentally determined to be linearly dependent over the range of ε studied (see manuscript Table 1), *i.e.* $C(\varepsilon) = a\varepsilon + b$, where a and b are respectively constants representing linear slope and intercept:

$$k_o(\varepsilon) = \varphi \cdot \frac{(a\varepsilon + b)^2}{(1-\varepsilon)} \quad \text{where } \varphi = \frac{32}{C_p P \pi \rho_{cryst} d^4} \tag{A.4}$$

Correction of k_o to k using manuscript Eq. (6) represents a constant offset term, c:

$$k(\varepsilon) = \varphi \cdot \frac{[a(\varepsilon) + b]^2}{(1-\varepsilon)} + c \tag{A.5}$$

and

$$k(f) = \varphi \cdot \frac{[a(1-f) + b]^2}{f} + c \tag{A.6}$$

Here, f is solid fraction (mathematical complement to ε, *i.e.*, $f = (1-\varepsilon)$), which is substituted for ease of expansion of Eq. (A.6):

$$k(f) = \varphi a^2 f + \varphi(a+b)\frac{1}{f} - 2a^2\varphi - 2ab\varphi + c \tag{A.7}$$

Eq. (A.7) can be re-written in the general form:

$$k(f) = Af + B\frac{1}{f} + C \tag{A.8}$$

where constants $A = \varphi \cdot a^2$; $B = \varphi \cdot (a+b)^2$; and $C = -2a^2\varphi - 2ab\varphi + c$. In order to determine these constants, assuming $k(f)$ and f are known from experimental data, Eq. (A.8) can be expressed in a quadratic form by rearrangement and multiplication by f:

$$Af^2 + [C - k(f)]f + B = 0 \tag{A.9}$$

Since $f = 1 - \varepsilon$, $k(\varepsilon)$ will also be quadratic, as demonstrated in manuscript Table 3.

References

[1] W.D. Callister Jr., Materials Science and Engineering: An Introduction, sixth ed., John Wiley & Sons, Inc., New York, 2003.
[2] M. Hu, D. Yu, J. Wei, Thermal conductivity determination of small polymer samples by differential scanning calorimetry, Polym. Test. 26 (2007) 333–337.
[3] Y. Lin, R.P. Cogdill, P.L.D. Wildfong, Informatic calibration of a materials properties database for predictive assessment of mechanically activated disordering potential for small molecule organic solids, J. Pharm. Sci. 98 (2009) 2696–2708.
[4] P.L.D. Wildfong, B.C. Hancock, M.D. Moore, K.R. Morris, Towards an understanding of the structurally based potential for mechanically activated disordering of small molecule organic crystals, J. Pharm. Sci. 95 (2006) 2645–2656.
[5] I.S. Buckner, R.A. Friedman, D.E. Wurster, Using compression calorimetry to characterize powder compaction behavior of pharmaceutical materials, J. Pharm. Sci. (2009), doi:10.1002/jps.21881.
[6] A. Zavaliangos, S. Galen, J. Cunningham, D. Winstead, Temperature evolution during compaction of pharmaceutical powders, Pharm. Tech. 97 (2008) 3291–3304.
[7] Y. He, Rapid thermal conductivity measurement with a hot disk sensor. Part 1. Theoretical considerations, Thermochim. Acta 436 (2005) 122–129.
[8] Y. He, Rapid thermal conductivity measurement with a hot disk sensor. Part 2. Characterization of thermal greases, Thermochim. Acta 436 (2005) 130–134.
[9] D.G. Cahill, M. Katiyar, J.R. Abelson, Thermal conductivity of a-Si:H thin films, Phys. Rev. B 50 (1994) 6077–6081.
[10] F. Yakuphanoglu, M. Sekerci, The crystallization kinetics and thermal conductivity of alumina/fluorescin sodium salt (Al_2O_3/FSS) composites, J. Phys. D: Appl. Phys. 38 (2005) 74–77.
[11] J. Chiu, P.G. Fair, Determination of thermal conductivity by differential scanning calorimetry, Thermochim. Acta 34 (1979) 267–273.
[12] C.P. Camirand, Measurement of thermal conductivity by differential scanning calorimetry, Thermochim. Acta 417 (2004) 1–4.
[13] M. Merzlyakov, C. Schick, Thermal conductivity from dynamic response of DSC, Thermochim. Acta 377 (2001) 183–191.

[14] G.L. Bennis, R. Vyas, R. Gupta, S. Ang, W.D. Brown, Thermal diffusivity measurement of solid materials by the pulsed photothermal displacement technique, J. Appl. Phys. 84 (1998) 3602–3610.
[15] J.S. Tse, M.A. White, Origin of glassy crystalline behavior in the thermal properties of clathrate hydrates: a thermal conductivity study of tetrahydrofuran hydrate, J. Phys. Chem. 92 (1988) 5011–5066.
[16] G. Hakvoort, L.L. van Reijen, A.J. Aartsen, Measurement of the thermal conductivity of solid substances by DSC, Thermochim. Acta 93 (1985) 317–320.
[17] M.Y. Keating, C.S. Mclaren, Thermal conductivity of polymer melts, Thermochim. Acta 166 (1990) 69–76.
[18] R.L. Blaine, S.M. Marcus, Derivation of temperature-modulated DSC thermal conductivity equations, J. Therm. Anal. 54 (1998) 467–476.
[19] E. Verdonck, K. Schaap, L.C. Thomas, A discussion of the principles and applications of Modulated Temperature DSC (MTDSC), Int. J. Pharm. 192 (1999) 3–20.
[20] S.M. Marcus, R.L. Blaine, Thermal conductivity of polymers, glasses and ceramics by modulated DSC, Thermochim. Acta 243 (1994) 231–239.
[21] ASTM, Standard Test Method for Thermal Conductivity and Thermal Diffusivity by Modulated Temperature Differential Scanning Calorimetry (E 1952-01) in Annual Book of ASTM Standards, vol. 14.02, ASTM International, West Conshohocken, 2001, pp. 1–6.
[22] B.-K. Jang, H. Matsubara, Influence of porosity on thermophysical properties of nano-porous zirconia coatings grown by electron beam-physical vapor deposition, Scripta Mater. 54 (2006) 1655–1659.
[23] B.-K. Jang, Y. Sakka, Thermophysical properties of porous SiC ceramics fabricated by pressureless sintering, Sci. Technol. Adv. Mater. 8 (2007) 655–659.
[24] S.R. Byrn, R.R. Pfeiffer, J.G. Stowell, Solid-State Chemistry of Drugs, second ed., SSCI-Inc., West Lafayette, 1999.
[25] F.H. Allen, The Cambridge Structural Database: a quarter of a million crystal structures and rising, Acta Crystallogr. B58 (2002) 380–388.
[26] I.J. Bruno, J.C. Cole, P.R. Edgington, M. Kessler, C.F. Macrae, P. McCabe, J. Pearson, R. Taylor, New software for searching the Cambridge Structural Database and visualizing crystal structures, Acta Crystallogr. B58 (2002) 389–397.
[27] D.A. Fletcher, R.F. McMeeking, D. Parkin, The United Kingdom Chemical Database Service, J. Chem. Inf. Comput. Sci. 36 (1996) 746–749.